International Conference
ENGINEERING MECHANICS 2010
Svratka, Czech Republic, May 10 – 13, 2010

TREATMENT OF EXTRA-ARTICULAR FRACTURE FOLLOWING TOTAL KNEE ARTHROPLASTY

J. Křen, L. Ondoková*, J. Matějka, K. Koudela, K. Koudela jr.**

Summary: *Fractures of distal femur following total knee arthroplasty (TKA) are infrequent, but devastating complications. They require anatomically stable internal fixation. The selection of suitable implant type, which could fixate the fractures of distal femur, is very important problem to solve in the orthopedic practice. This study deals with the fractures in extra-articular part of distal femur and it tries to suggest, which of four implants often used to treat this fracture type is most suitable to fixate the femoral bone. The previously developed FE leg model with implemented TKA was used. Four types of generated implant models were integrated into leg model to simulate the fracture treatment.*

1. Introduction

The biomechanical modeling has widely recorded significant development during the last years. Biomechanical models are used not only in the area of traffic for analyzing the effect of accident on human body, but also in the area of medicine, sport, army and leisure time. The medical problem from the orthopedic area: the treatment of simple extra-articular fracture of distal femur was solved in this study. Extra-articular fractures of distal femur following total knee arthroplasty (TKA) are infrequent, but devastating complications (Bezwada et al., 2004). Although the prevalence is low, ranging from 0.3% to 2.5%, the general population ages and the number of performed TKAs increases, and also the probability of the number of periprosthetic femur fractures rises (Bezwada et al., 2004; Ritter et al., 1995). The fractures of distal femur are divided into three groups, i.e. A, B and C. Extra-articular fractures of distal femur belong to the group A (Müller et al., 2007; Schewring & Meggitt, 1992). Its division is taken according to (Schewring & Meggitt, 1992) (Figure 1).

Presented fractures can result from relatively low energy loading for old people and from high energy loading for young people, respectively. Since fractures occurring after TKA are characteristic for predominantly older population, this study deals with the group of older people.

* Prof. Ing. Jiří Křen, CSc., Ing. Lenka Ondoková, Ph.D.: Department of mechanics; Fakulty of Applied Science; University of West Bohemia; Univerzitní 22; 306 14 Plzeň; tel.: +420.377 632 000, fax: +420.377 632 002; e-mail: kren@kme.zcu.cz

** Doc. MUDr. Jiří Matějka, Ph.D., Prof. MUDr. Karel Koudela, CSc., MUDr. Karel Koudela: University Hospital in Plzeň; alej Svobody 80, 304 60 Plzeň - Lochotín

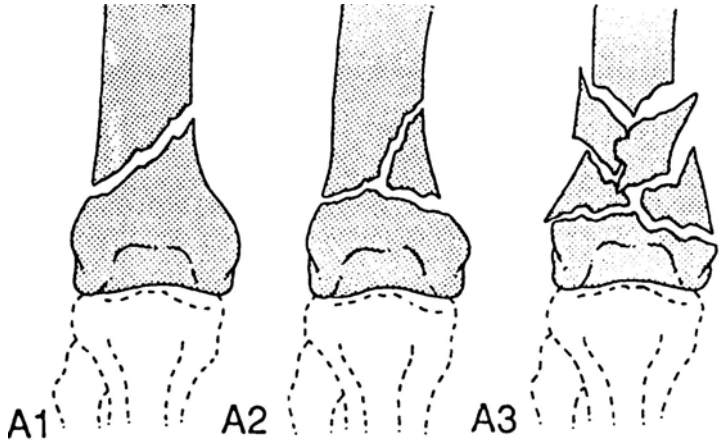

Figure 1 The division of distal femoral bone fractures in extra-articular part according to Schewring & Meggitt, 1995 (A1 - simple extra-articular fracture, A2 - metaphyseal wedge fracture and A3 - metaphyseal complex extra-articular fracture).

The treatment of simple extra-articular fractures is difficult, since it is influenced by quality of bone, fracture type, type of surgical implant and by whole disposition of the patient (Bezwada et al., 2004; Rabin, 2009). To capture all these facts in the model there is need to have many input data, which are difficult to obtain. Therefore there was made several simplifications: i) The attention was devoted to only one fracture type to the simple extra-articular fracture (A1), ii) Four models of often used implant types were created, iii) FE leg model was completed by material parameters corresponding to behaviour of average older man without any diseases.

Generally, distal femoral fractures require anatomically stable internal fixation for best treatment results and it usually needs the surgical intervention (Rabin, 2009). For this purposes the orthopedic surgeons used several implants, for example condylar plate, non-contact bridging plate, distal femoral nail, etc. (Müller et al., 2007). They are usually from anti-corrosive steel or titanium alloy. Not every kind of implants is suitable for each type of distal femur fractures (Johnson, 1988). The following problems may occur: a) the implant can rupture or deform, b) the inadequate fixation can cause further fracture of femoral bone, etc. In summary the chosen device must provide enough motionless fixation of femoral bone, which enables as fast patient motion as possible (Halpenny & Rorabeck, 1984).

This study arose in cooperation with Faculty Hospital in Plzeň in order to find, which of four often used implants is most suitable to treat A1 fracture. Otherwise the aim was to suggest, which implant ensure the sufficient bone fixation without apparent implant changes.

2. Methods

FE model of human leg with integrated TKA model developed previously at University of West Bohemia by Jansová et al., 2004; Křen & Hynčík, 2002; Pokorný, 2007 was used in this study. The models of four implants were created and consequently integrated into the leg model in Altair® HyperMesh® software. Whole model was completed and subsequently loaded. FE biomechanical simulations and analysis were performed in PAM-CRASH™ software (PAM-CRASH/SAFE™ Notes Manual, 2007).

2.1 Description of leg model

The leg model consists of femur, tibia, fibula, patella, four ligaments and two muscles (Figure 2). For the purpose of this study the femoral model had to be divided into two segments to simulate A1 fracture (Figure 2).

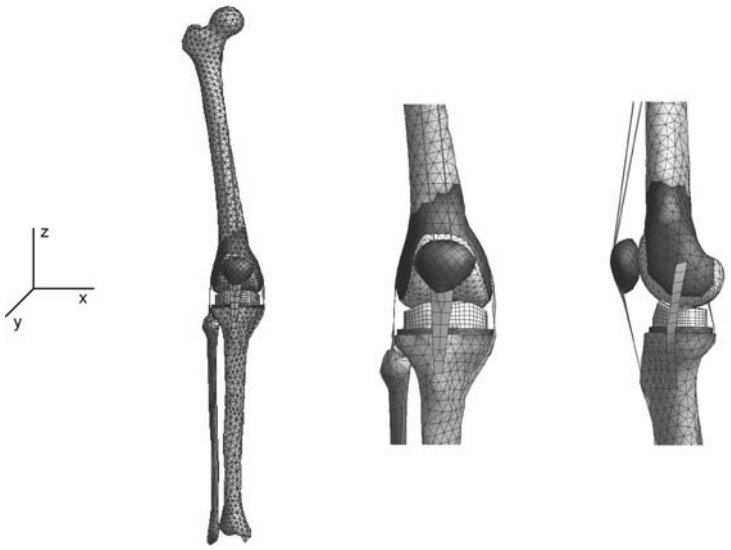

Figure 2 FE deformable model of leg with the fracture A1 in distal femoral part occurring after implementation of TKA.

All of leg bones, i.e. femur, tibia, fibula and patella, were modeled as deformable. Each bone model was divided into two parts. The first one representing the compact bone is modeled by tria shell elements. The second one representing the spongy bone is modeled by tetrahedral solid elements. The material properties completing the geometry of leg model were obtained from the previous works performed by (Křen et al., 2001; Pokorný, 2007). Since this study was devoted to the investigation of interaction of the femur and four types of implants, which are used to treat A1 fractures, the attention was predominantly paid to properties of femoral bone. Its material parameters were obtained from (Haug et al., 2004).

Generally, the bone tissue is usually considered to be orthotropic in biological reality. However, this behaviour is characterized by many parameters, which are difficult to obtain in biological reality and hence to define such material is rather complicated in the solver PAM-CRASH™ (PAM-CRASH/SAFE™ Notes Manual, 2007). In the studies (Křen & Hynčík, 2002), the comparison of femoral behaviour in case when the bone was modeled as orthotropic or isotropic is presented. It was found that the differences are negligible.

Therefore in this study, the isotropic behaviour of femoral bone was supposed. The elastic behaviour of shell elements was characterized by Young modulus, *E,* [GPa] and by Poisson ratio, *ν*, [-]. The elastic behaviour of the solid part was characterized by shear modulus, *G*, [GPa] and by bulk modulus, *K*, [GPa], which are described by Eq. (1) and (2).

$$G = E / 2(1+\nu), \tag{1}$$

$$K = E / 3(1-2\nu). \tag{2}$$

Since the mechanical properties of human bones change with age as a consequence of changes of density and mineral content (Burstein et al., 1976), the material properties of femoral bone of 70 year old man were taken into account. This is in agreement with the reality since the implementation of TKA and following possible femoral fractures are more often for older people. The average age of people affected by the fracture occurring after TKA is approximately 70 years (Ritter et al., 1995). Average femoral material properties of 70-year old man and corresponding reference are summarized in Tables 1 and 2.

Table 1 Material properties of femoral compact bone typical for 70 year old man.

	E [GPa]	v [-]	σ_y [GPa]	References
Femoral compact bone	16.3	0.28	0.111	Burstein et al., 1976

Table 2 Material properties of femoral spongy bone typical for 70 year old man.

	G [GPa]	K [GPa]	σ_y [GPa]	References
Femoral spongy bone	0.0231	0.050	0.018	Ciarelli et al., 1986

In this study only the elastic behaviour of femoral bone is supposed, since the plastic deformation of bones observed for children declines with increasing age because of decrease of the bone flexibility (Griffth et al., 2005) i.e. the plasticity is neglectable for older people. The yield stress is mentioned due to the implementation of the model to the solver PAM-CRASH™.

2.2 Description of implant models

There were created models of four implant types, which are commonly used by orthopedic specialists to treat A1 fractures. To obtain the implant measurements for geometry arrangement, there were performed several measurements by slide caliper. The meshes of individual implants were generated on personal computer in Altair®HyperMesh® software, which is a high-performance FEA pre-processor for popular finite element solvers. The implant meshes were created by predominantly hexahedral elements. Pyramid or tetrahedral elements were integrated in the place with no possibility to use the hexahedral ones. In case of implants from anti-corrosive steel the number of nodes and elements was approximately 4500 and 2500, respectively. In case of implants from titanium alloy the number of nodes and elements was approximately 8200 and 6000, respectively.

Two from the implants were made from anti-corrosive steel. In this study they are called steel implants. The other two were made from titanium alloy. They are called titanium implants.

The behaviour of implant was supposed as elasto-plastic with isotropic hardening (PAM-CRASH/SAFE™ Notes Manual, 2007). The elastic behaviour was characterized by bulk modulus, K, and by shear modulus, G. Plastic hardening was described by yield stress, σ_y,

[GPa] and by tangent modulus, E_t, [GPa]. Specific values of these parameters are summarized in Table 3.

Table 3 Material parameters of implants from anti-corrosive steel and titanium alloy, respectively.

	G [GPa]	K [GPa]	σy [GPa]	Et [GPa]
Steel implants	79.23	171.67	0.30	0.62
Titanium implants	42.31	91.67	0.26	0.50

The meshes of femoral bone and implants were merged together without any gaps in the bone, i.e. there is mesh of screws and bones in the same place (Figures 3, 4). However this negligible adding of bone mass very inappreciably influences simulation results. It was previously found that the results of simulation in the case of mesh with gap and without gap were practically same (Křen et al., 2001). The placement of implants inside the femoral bone was consulted with orthopedic surgeons.

2.2.1 Titanium implants

Titanium implants, which were investigated: i) Titanium Distal Femoral Nail (DFN) and ii) Non-Contact Bridging plate (NCB), are presented below.

DFN is solid titanium implant with widths between 9mm and 12mm. The nail differs in the length and proximal locking possibilities. The long nail with a length between 300mm and 420mm can be inserted with 2 proximal holes for static lateral locking and 1 long hole for dynamic anterior-posterior locking. To achieve optimal stabilization, there is preferred the longest and thickest nail (Walcher et al., 2000).

For the simulation there was used DFN with the length of 200mm. The model of DFN (Číhalová & Fryčová, 2007) and its placement inside the femoral bone affected by A1 fracture is visualized in Figure 3.

It belongs among the less invasive stabilization system (Erhardt et al., 2008). NCB is the next generation of the locking plate system for trauma surgery. Requiring a smaller than normal incision, there is less damage of surrounding soft tissue and a reduced risk of complications with wound healing. The NCB combines conventional plating technique with polyaxial screw placement and angular stability (Erhardt et al., 2008). Keeping the plate off the bone can reduce the potential for periosteal damage and periosteum blood supply impairment.

NCB plate for the left leg with 246mm in length was taken into account. Screws were placed on the both ends of the plate. This was consulted with orthopaedic specialists. Moreover one screw was used in the middle of plane. Its task is to stabilize the bone, because there was observed the movement of femoral bone in the place of fracture without them in the simulation results performed during this study.

The model of NCB (Číhalová & Fryčová, 2007) and its placement in the femoral bone model affected by the A1 fracture is visualized in Figure 3.

Figure 3 The model of DFN and NCB implants and their placement into the femoral model affected by fracture A1.

2.2.1 Steel implants

Steel implants, which were taken into account: I) Dynamic Compression Screw (DSC) and II) Condylar Plate 95° (CP), are presented below.

DCS is a metallic plate used in practice for internal fixation of bone, typically after fractures. The device consists of a lag screw and a side plate with a barrel. As the name implies, it is designed to exert dynamic pressure between the bone fragments to be transfixed. Dynamic compression is achieved either by attaching a tension device to a plate or by using a special dynamic compression plate.

The model of DCS and its placement in the femoral bone model affected by the A1 fracture is visualized in Figure 4.

Condylar Plate (Figure 4) has fixed angle (95°) between its blade and plate portion. The used plate length varies with the fracture pattern. The shortest blade is 50cm, and the length of the chosen blade depends on the size of the femur and whether the plate is being used in the distal or proximal femur.

This paragraph is devoted to the summary of the placement of implant into the femur. The screws of all implants had to go through the bone to the end of opposite bone side. No screw can be placed in the place of fracture. The screws are positioned along the whole length of steel plate. On the other side the screws are placed only at the ends of titanium plate and one or two screws are placed in the middle of plate for better implant stabilization.

Figure 4 The model of DCS and CP 95° implants generated in this study and its placement into the femoral model affected by fracture A1

2.2 Completion of models

All of implant models, which were integrated into femoral model, had to be fixed to the bone to prevent the movement of implants inside the femoral bone after loading. Two types of the contacts were used for the fixation of the implant models in the leg models: i) sliding contact and ii) tied contact. Both contacts are offered by the solver PAM-CRASH™ (PAM-CRASH/SAFE™ Notes Manual, 2007). These contact interfaces require the definitions of the "master" and the "slave" surfaces via the finite segments and nodes, which might get into the contact with each other during the simulation.

ad i) Sliding contact allows two parts to move with respect to each other (PAM-CRASH/SAFE™ Notes Manual, 2007). This type of the interface was used to simulate the mutual contact of individual plates and femoral compact bone. Further in certain cases it was used to define the connection of screws and plate, i.e. in the case of the absence of the threads on the plate. This screw fixation is no-angle stable and it is typical for dynamic compression screw plate and condylar plate.

ad ii) For the tied interface, the slave nodes can be positioned at a certain distance to the master surface. This type of contact interface was used to simulate the footing of screws inside the femoral bone. For this purposes the net of shell elements of negligible mass inside the femoral bones was created, because the slave nodes can be tied only to the shell elements. Further, this type of contact interface was used to model the connection of screws and plates in such cases, where the threads are presented. This screw fixation is angle stable and it is characteristic for non-contact bridging plate.

No-angle stable fixation causes the movement of the screws inside the plate after loading. On the other side the movement of the screw inside the plate with angle stable fixation is impossible. The situation is visualized in Figure 5.

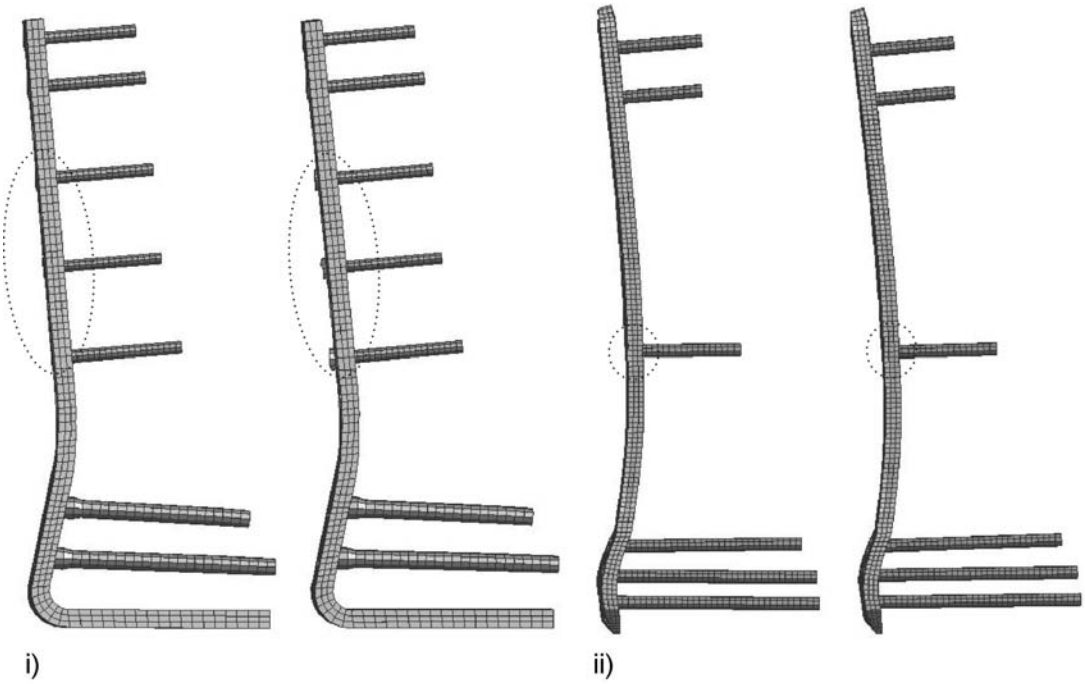

Figure 5 i) No-angle stable fixation of CP 95° in the initial state and after loading from the top, ii) angle stable fixation of NCB in the initial state and after loading from the top. Notice that no-angle stable fixation of CP 95° causes the screw drawing-out after loading

2.3 Biomechanical simulations

The solver PAM-CRASH™, which is a dynamic explicit method structure analysis program developed by ESI Group (Engineering Simulation for Industry), was used to complete models and for following biomechanical simulations.

Because of the size of bone and implant elements, the time step was too small, i.e. approximately 10^{-4} ms for the implants and 10^{-3} ms for the bones. This fact caused the long computing time. Therefore the scaling of model stiffness and mass was used (PAM-CRASH/SAFE™ Notes Manual, 2007). This possibility is offered by the solver, which after finding that the time step is too small, adjusts internal element parameters to obtain the stable time step. This scaling can be only used in the case when the static loading without gravity using is applied. Therefore there could not be applied dynamical loading, which represents the process of leg loading during walking. Thus only quasistatic loading corresponding to the femur loading arising during one foot stand, which is one phase of walking, could be used. However, when the scaling is used, the inertial forces, which cause the vibration of the system, arise. On that account there was used the damping of inertial forces, which is offered by the solver (PAM-CRASH/SAFE™ Notes Manual, 2007).

The damping for each node, which is proportional to the added mass, is described by Eq. (3)

$$f_i = - m_i q_{crit} v_{i,,} \tag{3}$$

where *fi* [kN] is internal nodal damping force, q_{crit} [(ms)$^{-1}$] critical damping and v_i [mm(ms)$^{-1}$] is nodal velocity vector (PAM-CRASH/SAFE™ Notes Manual, 2007).

Critical damping of, for example, a single-degree-of-freedom vibration system with circular frequency ω is obtained from Eq. (4)

$$q_{crit} = 2\omega = 4\pi / T, \tag{4}$$

where T [(ms)] is the period of vibration, which can be used to calculate q_{crit}.

In the case of biomechanical simulations, where T = 100 000 (ms), q_{crit} equals to approximately 0.000 126 (ms)$^{-1}$. As it was found from the results of simulations the model converged to the steady state in all cases during the first 50 000 (ms).

In all presented simulations the leg was loaded from the top in the direction of Z axis by a nodal force corresponding to the femur loading during one foot stand. The value of this nodal force was obtained from Rybka. & Vavk, 1993, where the size of femoral-tibia force acting on the knee joint during various types of movements was compared (Table 4).

Table 4 The loading of knee joint during one foot stand (BM is body mass [kg], i.e. the mass of human body Rybka & Vavk, 1993.

	Femoral-tibial force [multiplication of BM]
Walking on plane	4.3
Walking upstairs	4.9
Walking up the hill	4.4
Walking on plane	4.3
Walking upstairs	4.9
Walking up the hill	4.4

Under the assumption that the femoral bone yields to plastic deformation minimally after loading, it can be said that the loading applied on the upside of femur is comparable to the femoral-tibia force acting in the knee joint. Hence the parameter 2.8 was used to load the femur from above.

To load the model there was supposed the mass of average adult man, i.e. the man with the mass of 75kg. Hence the nodal force acting on the upside of the femoral bone was (2.80*75.00*9.81)N = 2.06kN. This value of the nodal force was used to load the femoral bone model with four types of implants treating A1 fracture of distal femur. The bottom part of the leg model, i.e. the bottom parts of the tibia and fibula bone, were fixed.

In this study with the aim to show, which of four presented implants is the most suitable to treat the simple extra-articular fracture of distal femur, FE analysis of all simulations with various types of implants was performed. To analyze biomechanical simulations the individual implant von Mises stress, which is characterized by Eq. (5), was investigated (Figures 6, 7, 8, 9). This comparative stress takes into account all occurring stresses in the three directions of the coordinate system.

$$\sigma = \sqrt{3(\sigma_{xy}^2 + \sigma_{yz}^2 + \sigma_{xz}^2) + \sigma_{xx}^2 + \sigma_{yy}^2 + \sigma_{zz}^2 - \sigma_{xx}\sigma_{yy} - \sigma_{yy}\sigma_{zz} - \sigma_{xx}\sigma_{zz}}\ , \quad (5)$$

where σ_{xx}, σ_{yy}, σ_{zz} are the normal stresses [GPa] and σ_{xy}, σ_{yz}, σ_{xz} are the shear stresses [GPa].

Values of von Mises stresses were computed by the solver automatically. Since this objective was computationally demanding, the problem was not solved on the personal computer but on the Linux cluster.

3. Results

There was found that till 50s the model of the leg with implemented TKA and affected by the A1 fracture, which is treated by various types of implants, converged to stable state. Hence the comparisons of von Mises stress distributions for four generated models with various implant types in the time of 50s are presented.

3.1 Titanium distal femoral nail

The von Mises stress of screws increases minimally. In the case of locking screw and spiral blade the stress grows maximally to 90MPa. In the case of the nail the situation was different. In one-third of the length, where the nail narrows, the center of stress distribution could be observed (Figure 8). The stress increased to 190MPa in this place.

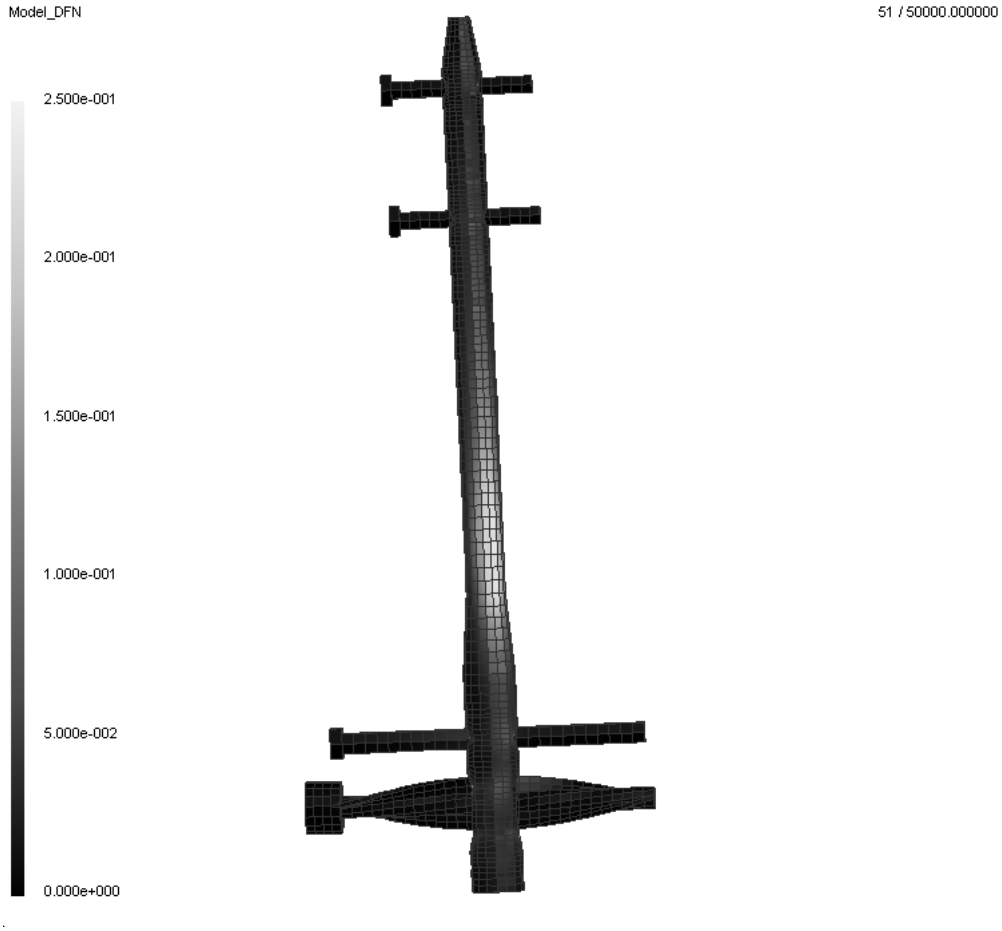

Figure 6 von Mises stress [GPa] of DFN implant model after loading in 50 000 (ms)

3.2 Non-contact bridging plate

The von Mises stress of screw increased minimally in one-half of the length and in the end. However, in the places where the screws leave the plate the stress grew to 100MPa. Concerning the plate there could be observed the increase of stress around the one-half of the length in the concave part. There the stress grew to 130MPa (Figure 7).

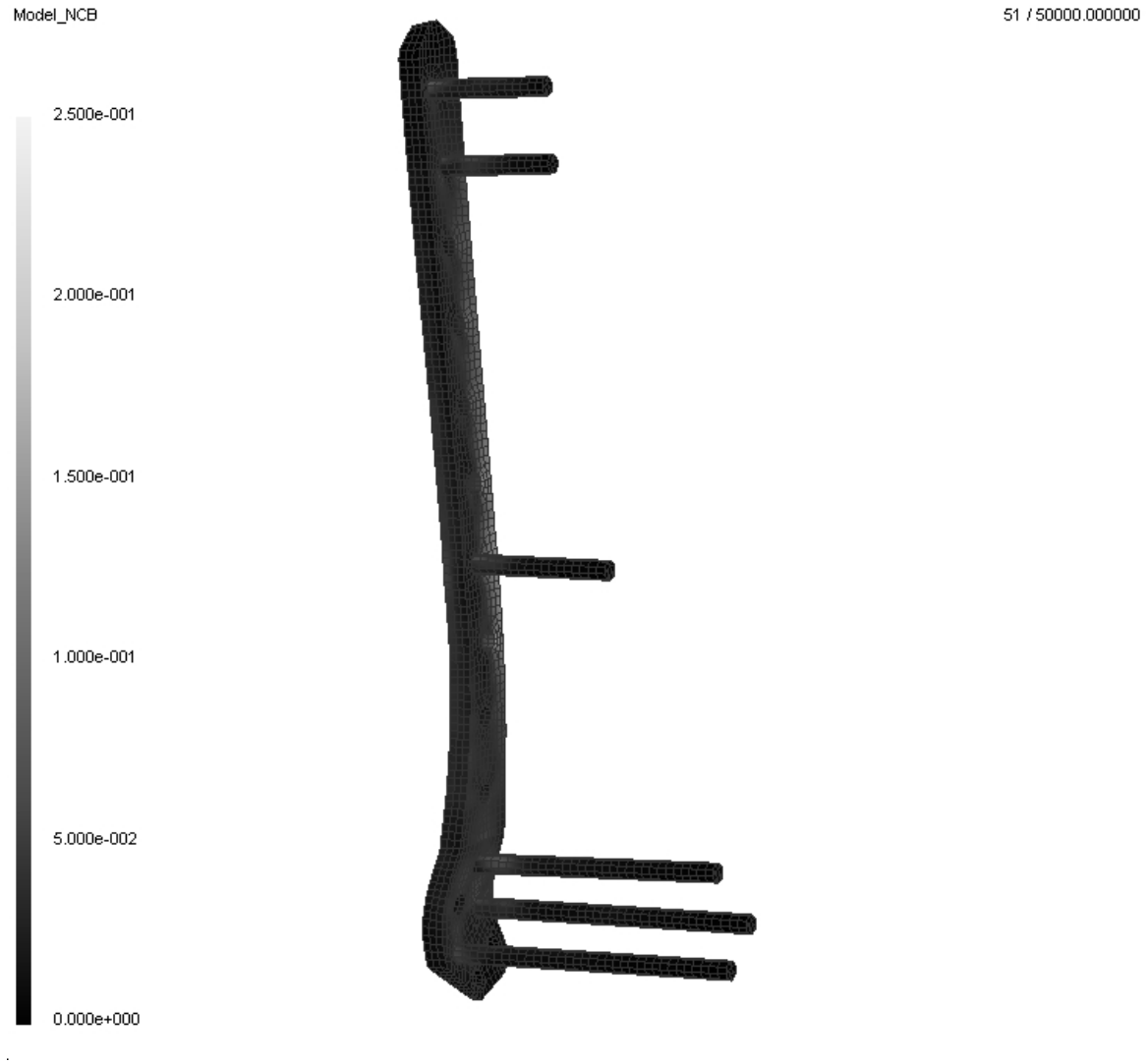

Figure 7 von Mises stress [GPa] of NCB implant model after loading in 50 000 (ms)

3.3 Dynamic compression screw

There can be observed small increase of von Mises stress along the plate length. Accumulation of stress can be observed around the dies for screws, in the places where the screws are presented. This stress was around the 250MPa. In the case of screws there was minimal increase of von Mises stress in the half-length and in the end of the screw. On the other side in the head of screw and the area, where the screw leaves the plate, von Mises stress was 250MPa (Figure 8).

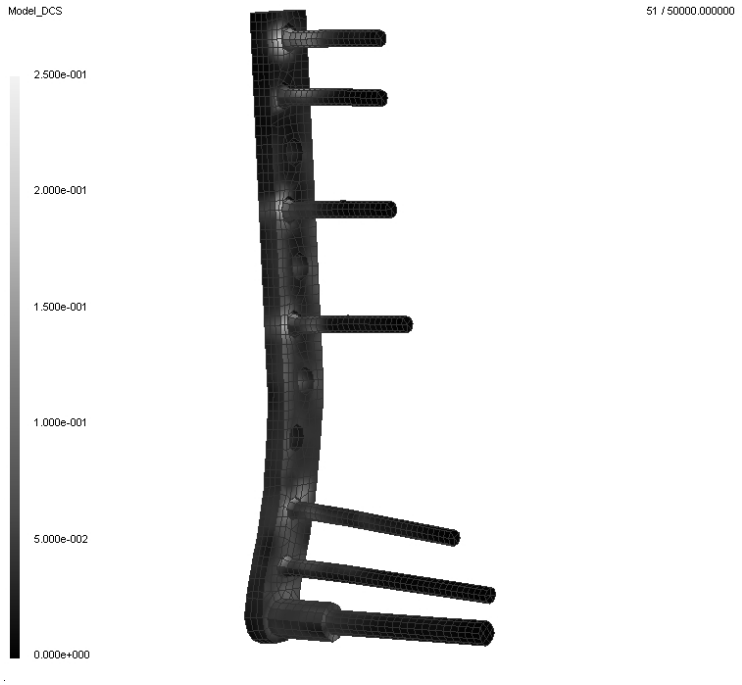

Figure 8 von Mises stress [GPa] of DCS implant model after loading in 50 000 (ms)

3.4 Condylar plate

The stress of the screws was concentrated in the place where the screws leave the plate and subsequently declined to one-half of the length in case of short screw and to three-fourth in case of longer screw. Maximal stress could be observed in the heads of fourth and fifth screw from the top, where the stress reaches to 240MPa. Concerning the plate stress it increased minimally along the plate length. More apparent growth of stress was in the plate die around the screws. Here the stress increased to 240MPa (Figure 9).

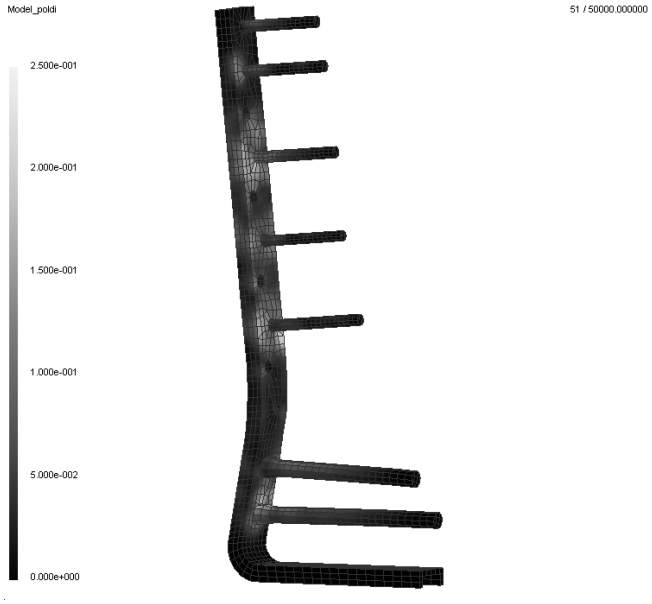

Figure 9 von Mises stress [GPa] of condylar plate model after loading in 50 000 (ms)

4. Discussion

Computer simulation based on FEM can provide sufficient information to characterize the behaviour of implants, which are used to treat the extra-articular fracture of distal femur.

The previously developed FE model of leg was used for this study. Newly created four types of implants, i.e. distal femoral nail, non-contact bridging plate, dynamic compression screw and condylar plate, were integrated into leg model. There was taken into account that some screws are angle stable and some screws are no-angle stable. This situation was simulated by two types of contact: i) tied contact to simulate angle stable fixation and ii) sliding contact to simulate no-angle stable fixation. Both contacts are offered by the solver PAM-CRASH™ (PAM-CRASH/SAFE™ Notes Manual, 2007).

Due to small computation time step there was used the mass and stiffness scaling of whole model. However these scaling causes the rise of inertial force, hence the damping to each node had to be applied.

To simulate the maximal femoral loading during walking on plane, the top of femur was loaded by the quasistatic nodal force corresponding to femoral loading during one foot stand. The bottom of tibia and fibula was fixed to constraint the displacements and rotations in all directions.

To analyze the behaviour of four implants after quasistatic loading, von Mises stress distribution of individual implants was investigated. The results are visualized in Figures 6, 7, 8, 9. It was found that implants from anti-corrosive steel, i.e. dynamic compression screw and condylar plate, are very stable after the loading. The stress is concentrated around the holes in the plate and in the heads of screws. This lead, in case of big loading, to the plastic deformation of the head screws, which could lead to rupture of screws in places, where the screws leave the plate. Concerning the implants from titanium alloy, i.e. distal femoral nail and non-contact bridging plate, the situation was following. In case of distal femoral nail the stress was concentrated at thinning of the nail. This could cause very probably the rupture of the nail in this place. This corresponds with the reality, when it was found that the patients with this type of implants underwent the rupture in the place, which corresponds to the maximal distribution of von Mises stress obtained during simulation. The non-contact bridging plate, which has as the only one the angle stable fixation of screws, seems to be very stable. The stress increases in the half length of the plate in the inner concave side. However this increase is very small in the comparison with other implant types. Hence, on the base of FEM simulations, it seems that the non-contact bridging plate is the most suitable type of implant, which can be used to treat the simple extra-articular fracture of distal femur. Moreover, this implant has additional advantages. It is light, since titanium alloy is lighter than anti-corrosive steel. The placement of screws inside the plate is angle-stable, which ensures no movement of screws after loading, i.e. better possibility to heal the bone. Moreover its use is less invasive for patient, since there is used only minimal amount of screws. Screws are usually used in the end of plates and only one or two in the center of plate. As it was found from the simulation results, these central screws restraint the movement of femoral bones in the place of fractures.

The conclusions were done for the simple extra-articular fracture of distal femur. The situation for metaphyseal wedge fracture (A2) (Figure 1) was investigated in study (Číhalová et al., 2009). The last from this group of fractures metaphyseal complex extra-articular fracture (A3) (Figure 1) will be solved in the future.

5. Conclusion

The behaviour after loading of four implants, which are used to treat simple extra-articular fractures of distal femur, was investigated by finite element simulations using the deformable model of human leg with implemented TKA. The femur was loaded by the quasistatic nodal force corresponding to the maximal loading during walking of average man. Two types of anti-corrosive steel implants and two types of titanium-alloy implants were used. It was found that the titanium-alloy implant the non-contact bridging plate is most resistant to the loading and so it can ensure enough fixation of simple extra-articular fracture of distal femur.

6. Acknowledgement

This study was supported by research project MSM 4977751303 and by research project IGA MZ No. NS-9726.

7. References

Altair® HyperMesh® 7.0 http://www.altair.com

Bezwada, H. P.et al. (2004) Periprosthetic supracondylar femur fractures following total knee arthroplasty. *Journal of Arthroplasty*, 19, 4, pp. 453-458.

Burstein, A. H. et al (1976) Aging of bone tissue: Mechanical properties. *Journal of Bone and Joint Surgery*, 58, 1, pp. 82-86.

Ciarelli, M. J. et al. (1986) Experimental determination of the orthogonal mechanical properties, density, and distribution of human trabecular bone from the major metaphyseal regions utilizing material testing and computed tomography. *Trans. Orthop. Res. Soc*., 16 , pp. 42-49.

Číhalová L. & Fryčová, D. (2007) Biomechanical model of the treatment of supracondylar femur fractures. *Proceedings of The 1st Young Researchers Conference on Applied Sciences*, pp. 105-110.

Číhalová L., Křen, J., Matějka, J. & Koudela, K. (2009) FE model of metaphyseal wedge fracture fixation in extra-articular part of distal femur. *Modelling and optimization of physical systems*, 1, 8, pp.11-16.

Erhardt, J.et al. (2008) Treatment of periprosthetic femur fractures with the non-contact bridging plate: a new angular stable implant. *Archives of Orthopaedic and Trauma Surgery*, 128, 4 , pp. 409-416.

Grifth, J. F., Tong, P. M., Hung, H. Y. & Kumta, S. M. (2005) Plastic Deformation of the Femur: Cross-Sectional Imaging. *American Journal of Roentgenology*, 184, pp. 1495-1498

Halpenny, J. & Rorabeck, C.H. (1984) Supracondylar fractures of the femur: results of treatment of 61 patients. *Canadian Journal of Surgery,* 27, 6, pp. 606-609.

Haug, E., Choi, H. Y., Robin, S. & Beaugonin, M. (2004) Human models for Crash and Impact Simulation. *Special Volume of Handbook of Numerical Analysis,* 12, pp. 231-670

Jansová, M., Hynčík, L., Horák, M. & Křen, J. (2004) Total knee replacement model. *Proceeding of Computational Mechanics*, pp. 172-182.

Johnson, E.E. (1988) Combined direct and indirect reduction of comminuted four-part intraacrticular T-type fractures if the distal femur. *Clinical Orthopaedics and Related Research*, 231, pp.154-162.

Křen, J. & Hynčík, L. (2002) Stability of proximal femur nail fixating per-trochanteric fracture. *Proceeding of Computational Mechanics*, pp. 219-224.

Křen, J., Hynčík, L. & Řehounek, L. (2001) Modelling of interaction between femur and PFN. *Proceeding of Computational Mechanics*, pp. 141-146.

Müller, M. E., Nazarian, S., Koch, P. et al. (1990) *The comprehensive classi_cation of fractures of long bones*, (Berlin Heidelberg New York, Springer Verlag).

PAM-CRASH/SAFE™ Notes Manual, Version 2007.

Pokorný, J. (2007) The patellofemoral joint and the total knee replacement. *Proceeding of Applied and Computational Mechanics*, pp. 595-602.

Rabin, S.I. (2009) Supracondylar femur fractures

http://www.emedicine.com/orthoped/topic319.htm.

Ritter, M. A., Keating, E. M., Faris, P. M. & Meding, J. B. (1995) Rush rod fixation of supracondylar fractures above total knee arthroplasties. *Journal of Arthroplasty*, 10, 2, pp. 213-216.

Schewring, D. J. & Meggitt, B. F. (1992) Fracture of the distal femur treated with the AO dynamic condylar screw. *Journal of Bone and Joint Surgery*, 74, 1, pp. 122-125.

Rybka, V. & Vavk, P. (1993) *Aloplastika Kolennho Kloubu*, (Arcadia).

Walcher, F., Frank, J. & Marzi, I. (2000) Retrograde nailing of distal femoral fracture – clear and potential indications. *European Journal of Trauma*, 4, pp. 155-168.